ACTA TECHNICA CORVINIENSIS – Bulletin of Engineering | e–ISSN: 2067 – 3809
Tome XVIII [2025] | Fascicule 1 [January – March]

[1.]M.C. IBEKWE, [2.]F. ALAPA, [3.]M.C. CHUKWU

DESIGN OF A MULTILAYER UWB MIMO PATCH ANTENNA FOR 5G MOBILE APPLICATIONS

[1.] Electronics and Telecommunications Engineering Department, Faculty of Engineering, Ahmadu Bello University, Zaria, Kaduna, NIGERIA.
[2, 3] National Space Research Development Agency, Abuja, NIGERIA

Abstract: Several performance metrics on radiation pattern management, gain, mutual coupling, bandwidth enhancement, size restriction, integration problems, and cost-effective manufacturing must be considered while designing antennas for 5G applications. Due to multipath radio signal propagation, 5G radio communications experience multipath fading. The MIMO technique and UWB technology are combined to address the bandwidth augmentation and multipath fading problems. Using the space diversity technique, a compact multiple input and multiple output patch antenna is proposed to mitigate signal attenuation due to multipath fading. The antenna is an improvement on an earlier design and it is constructed with multiple layers of different dielectric substrates (RO3035 and RO4350B). These layers are stacked vertically with lateral displaced radiating patches for bandwidth enhancement. The antenna is designed using advanced computer simulation technology from the microwave studio. This antenna system targets 5G operating bands ranging from 3 GHz to 11 GHz. The total structure size of the antenna is 16.7 x 16.7 x 2.53 mm^3. Simulated results have been presented and show the multilayer structure multiple-input multiple-output antenna has a 97.5 % bandwidth percentage improvement, 24.4% isolation improvement, and 79.75% size reduction when compared with the original design

Keywords: 5G; Multiple-input Multiple-output (MIMO); Ultra-wideband (UWB); Bandwidth; Multipath fading

INTRODUCTION

The demand for high data rates, enhanced connectivity, and improved spectral efficiency has become increasingly paramount in the rapidly evolving wireless communication landscape. Information and communication technology has rapidly evolved over the past decades. This is due to a shift from the original voice-centric/wired technology to wireless multimedia applications [1].

As industries transition towards advanced technologies such as the Internet of Things (IoT), smart cities, and autonomous systems, the existing communication frameworks are being challenged to support the burgeoning data traffic and diverse applications [2]. To bridge the convergence of digital wireless networks and the internet, there is a need for higher data rates, lower latency network access, and improved energy efficiency implementation [2]. The prerequisite to move from LTE to 5G wave systems is imperative.

In this context, Ultra-Wideband (UWB) and Multiple Input Multiple Output (MIMO) technologies have emerged as critical enablers for next-generation communication systems, particularly fifth-generation (5G) networks.

Recently, many scientific studies have been accomplished to shift from UHF spectrum bands (300 MHz to 3 GHz) to the 5G bands such as (6.0–7.9) GHz, (27.5–28.35) GHz, (37.6–40) GHz, and others [3]. However, the multipath propagation challenges in a rich scattering environment for such a high band lead to multipath fading. 5G systems rely on UWB and MIMO technologies for communication link reliability and high throughput [4]. Multiple antennas are employed in MIMO systems to overcome multipath fading, improve channel capacity, and ensure link quality.

UWB technology, characterized by its ability to transmit signals over a wide frequency spectrum, offers numerous advantages that align with the needs of modern communication systems. Unlike traditional narrowband systems operating over limited frequency ranges, UWB can utilize frequencies from 3.1 to 10.6 GHz, facilitating high data transmission rates and robust performance in multipath environments [5]. Moreover, UWB's inherent ability to coexist with other wireless technologies minimizes interference, allowing multiple devices to operate simultaneously without degrading overall system performance [6]. This feature is essential in densely populated urban

areas where numerous devices compete for a limited spectrum. Additionally, UWB's low power consumption makes it an attractive option for battery-powered applications, prolonging device lifespan and reducing the need for frequent recharging.

MIMO utilizes multiple antennas at both the transmitter and receiver ends to improve data throughput and reliability. By leveraging spatial diversity, MIMO can transmit multiple data streams simultaneously, effectively multiplying the capacity of a communication channel without requiring additional bandwidth [7]. This capability is particularly critical in 5G applications, where the demand for high-speed data and seamless connectivity is ubiquitous.

The integration of UWB and MIMO technologies represents a synergistic approach to addressing the challenges faced by contemporary communication systems. Antennas serve as the primary interface between the wireless environment and communication devices, and their design directly impacts the overall performance of the network. MIMO antennas have been investigated widely in recent years. Various decoupling structures were used to improve isolation, which is an important parameter of MIMO antennas [8]. Constraining mutual coupling in a narrow-band antenna is relatively straightforward, but the greatly increased degrees of freedom in a wideband one make it very challenging in such a case, especially if the size is also constrained. Several past studies have attempted to address this problem, with varying degrees of success [9 – 11].

To overcome the many drawbacks in previous designs, this paper combines the design concept for mutual coupling reduction and bandwidth enhancement [12,13] to propose a multilayer structure UWB MIMO patch antenna for 5G application. The multilayered approach allows for enhanced performance through improved isolation between antenna elements, reduced interference through the MIMO diversity Scheme, and optimized radiation patterns.

The remaining part of this paper is organized as follows: Section 2 provides literature reviews on the design of UWB MIMO patch antenna having different dielectric substrates, along with mathematical models related to the proposed scheme. Section 3 delves into the methodology employed in achieving the research objectives. Section 4 discusses the simulation and results obtained. Finally, Section 5 offers the concluding remarks for the entire research work.

RELATED WORKS

In [14], a dual-band microstrip patch antenna is designed to operate efficiently at frequency ranges of 3.32 GHz – 3.62 GHz and 4.72 GHz – 6.83 GHz. The microstrip configurations incorporate a rectangular patch with two slots on the FR4 substrates to achieve the antenna's dual-band performance. The overall size of the antenna is 19.141 x 25.33 x 1.6 mm^3, with a reflection coefficient of -5 dB at the lower frequency range, a gain of 2.3 dB and a radiation efficiency of 0.742. At the higher frequency range, a gain of 3.1 dB, a radiation efficiency of 0.7 and a reflection coefficient of -20.5 dB were achieved. The antenna is suitable for contemporary wireless communication and multi-frequency applications, but it also exhibits low gain and poor reflection coefficient suggesting potential impedance mismatch, leading to increased power loss due to reflections.

The research work of [15] proposed a closely packed wideband MIMO antenna operating in the frequency range of 4.5 GHz – 8.5 GHz. This bandwidth is achieved with multiple layers of substrates with different dielectric constants. The antenna has a compact size of 18.5mm by 18.5mm and achieves isolation of – 18 dB between the input ports. The parasitic elements are laterally displaced and driven by a main radiating patch through proximity coupling to improve isolation between elements. A multi-fidelity surrogate model-assisted design is used to optimize the antenna performance. R03006C and R04006 are the substrates used for fabrication. The antenna can be orthogonally configured or placed back-to-back for compactness. The proposed antenna is suitable for Sub-6 GHz 5G applications but cannot provide the ultra-high data speed of 5gbps due to bandwidth limitation.

Ref [16] proposed the design of a T-shape slot antenna for a sub-6 GHz 5G application. The antenna operates at two frequency bands of 5.923 GHz and 7.444 GHz respectively. The design is based on a T-shaped slot and a rectangular patch radiator that has been carefully optimized to achieve dual-band resonance. ROGERS RO4450B substrate is used as the dielectric material and a microstrip line feed powers the antenna. The CST software is used for the simulation. The results show that the antenna Gain and VSWR results are 5.45 dB and 1.049 at 5.933GHz; and 4.158 dB and 1.272 at

7.443 GHz respectively. The proposed antenna is susceptible to interference from other narrow bands due to its high-power spectral density of 16 W/m^2.

In [17], two dual-band rectangular microstrip patch antennas with an inset-fed technique are designed to provide the frequency bands of (3.3 GHz – 4.2 GHz)/ (3.3 GHz – 3.8 GHz) for Antenna 1 to operate at the sub-6 GHz and 5.9 – 7.1 GHz for Antenna 2 to operate at the sub-7 GHz. Slots were employed in Antenna 1 while Antenna 2 adopted a parasitic strip. FR-4 substrates with a relative permittivity of 4.3 was used as the dielectric material. The simulation was conducted using CST-MWS 2022 software-based simulations. Antenna 1 exhibited a bandwidth of 160 MHz at 3.45 GHz with a gain of 2.83 dBi while Antenna 2 had a bandwidth of 220 MHz at 5.9 GHz with a gain of 0.576 dBi. The proposed Antennas have bandwidths below 500 MHz which falls below the requirement for ultra-wideband application to provide the ultra-high data speed of 8gbps for 5G wireless communication.

In [18], a wideband MIMO array antenna comprising eight E-shaped and inverted I-shaped slots is proposed for a 5 G smartphone to operate with a frequency range of 3.3 GHz to 5 GHz. To boost the element shielding of the MIMO antenna system, a single-ended spanner-shaped slot is itched between each antenna element to achieve an isolation of 20 dB. Bandwidth enhancement is achieved by adjusting the E-shaped slots. The antenna has an ECC below 0.05 and an efficiency of 69%. The proposed antenna is suitable for sub-6 GHz applications and may not be suitable for the ultra-wideband applications of most 5 G networks.

Ref. [19] proposes a compact Multiple Input Multiple Output (MIMO) antenna system with high isolation for wireless applications in 5G connected devices. The antenna uses two decoupling methods which are Neutralization and Defected Ground Structure (DGS) to ensure the diversity of the proposed MIMO antenna. The DGS is achieved by engraving rectangular and L-shaped slots on the ground plane. Thus, the resulting antenna size is 92 × 88 mm^2 and consists of two elliptical antennas symmetrically arranged next to each other and space 0.47 wavelength apart. These configurations, dedicated to covering the 3.4 GHz -3.8 GHz have satisfactory Isolation performances of more than -30 dB in terms of reduction of mutual coupling between the antennas constituting the system. The antenna also demonstrates acceptable MIMO diversity parameters, such as Envelope Correlation (ECC), Diversity Gain (DG), and total efficiency. However, the proposed antenna has a narrow bandwidth of 0.4 GHz and may not provide the extreme data rate required for massive MIMO systems.

ANTENNA SUITABLE FOR 5G NETWORKS

5G networks operate at a wide range of frequencies, from sub-6 GHz to millimeter waves [20]. This means that antennas for 5G networks need to have a wide bandwidth, radiation pattern control, small size, and able to handle high frequencies. Also, 5G networks use MIMO technology to improve data rates and reliability [20]. Thus, the key performance characteristics of an antenna that makes it suitable for 5G networks include wide bandwidth to support different frequency bands, high gain to amplify the signal and improve the range of the network, radiation pattern control, efficiency, and polarization [18]. The most common antenna used in 5G networks is the patch antenna because of its low profile, low cost, size, weight, and ease of integration into other RF circuits [3]. Antennas play a crucial role in the performance of 5G networks. By carefully designing an antenna to achieve the desired performance characteristics using a multilayer structure and microstrip line connected to a Via traversing through the layer, drawbacks such as narrow bandwidth, surface wave loss, and mutual coupling can be greatly mitigated. A multilayer patch antenna is proposed for this research work because of its advantages such as very low profile, ease of integration into other RF circuits, low cost, and simplicity in creating arrays.

ANTENNA DESIGN CONCEPT

The processes involved in designing a UWB MIMO patch antenna having a multilayer structure began with the antenna parameter selection and the design equations, patch elements design, substrate selection, ground plain design, and feedline design. The antenna structure and arrangement are shown in Figure 1 and Figure 2. The design concept adopted from [15] uses two dielectric substrates of different thicknesses and permittivity to create a six-layer patch antenna structure. Four radiating square patches are laterally displaced on the top layer for bandwidth enhancement. The patches are parasitically excited by a driven square patch placed on the second layer. A

connection Via traversing through layer two ensures optimal impedance matching.

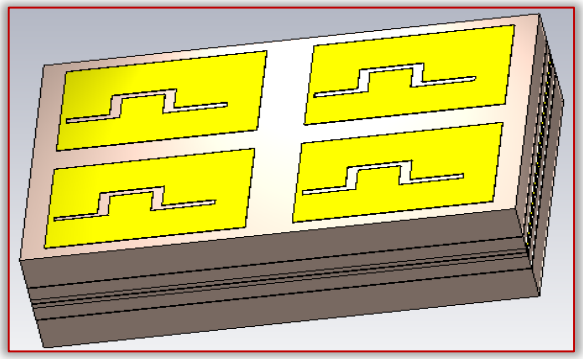

Figure 1. The Compact UWB MIMO Patch Antenna

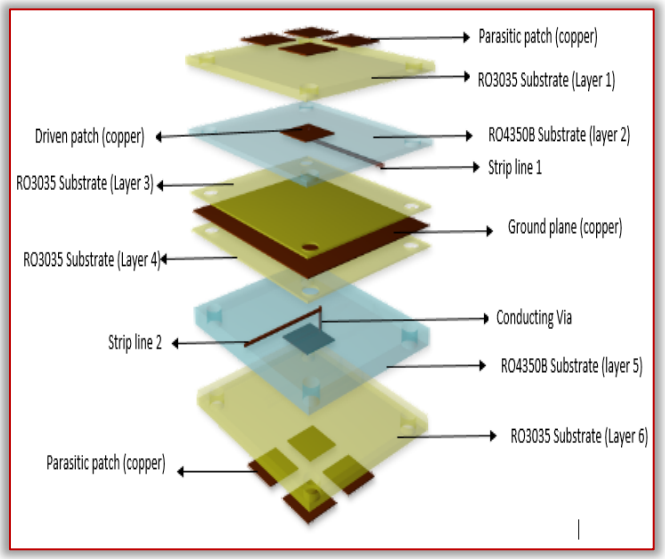

Figure 2. The UWB MIMO Patch Antenna Stacked Structure

Patch Dimension Calculation

The original antenna geometry consists of a single large parasitic squared-shape patch whose dimension is derived from Equation (1), Equation (2) and Equation (3) to operate at a center frequency of 5.74 GHz [21].

$$W_p = \frac{C}{2f_o\sqrt{\frac{E_r+1}{2}}} \quad (1)$$

where C is the speed of light (3.0 x 10^8 m/s), f_o indicates the center frequency, $\varepsilon_r$is the dielectric constant of the substrate and W_p indicates the width of the patch antenna.
The effective dielectric constant ε_{eff} is introduced in Equation (2) to account for the fringing and the wave propagation in the line. It can also be defined as the dielectric constant of the uniform dielectric material with a value range of $1 \leq \varepsilon_{eff} \leq \varepsilon_r$ [21].

$$\epsilon_{eff} = \frac{\epsilon r+1}{2} + \frac{\epsilon r-1}{2}\left[\frac{1}{1+12\sqrt{\frac{h}{W_p}}}\right] \quad (2)$$

where ε_{eff} is the effective dielectric constant, h is the substrate's height or thickness and W_p is the width of the patch.
Therefore, the length of the patch is calculated using Equation (3).

$$L_p = \frac{c}{2f_0\sqrt{\epsilon_{eff}}} - 0.824h\left[\frac{(\epsilon_{eff}+0.3)\left(\frac{W_p}{h}+0.264\right)}{(\epsilon_{eff}-0.258)\left(\frac{W_p}{h}\right)+0.8}\right] \quad (3)$$

where L_p is the length of the single parasitic patch. A square-shaped patch was selected for this multilayer UWB patch antenna design. The patch length was selected as the dimension of the square-shaped patch to consider the fringing effects which give rise to the fringing field.

Ground Plane Calculation

The dimensions of the ground plane are determined using Equations (4) and (5) from [22].

$$L_g = L_p + 6h \quad (4)$$

$$W_g = W_p + 6h \quad (5)$$

Using the mathematic model equations in [21] and [22], Fig. 2 shows the initial dimension of the squared-shape parasitic patch.

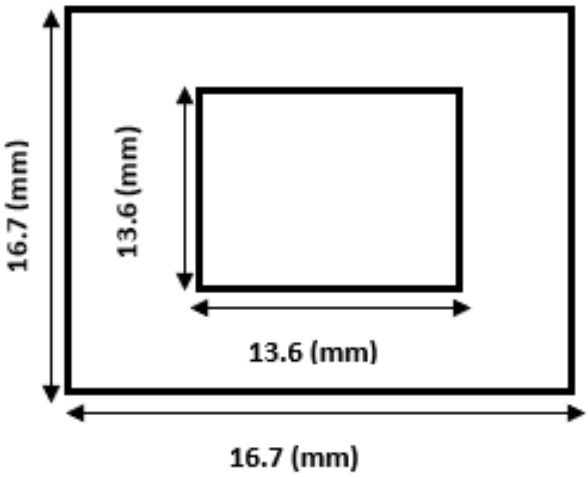

Figure 3. Initial Parasitic Square Patch

Using the design concept in [20], the single squared-shape parasitic patch is divided into four smaller squares of equal dimension 6.5 x 6.5 (mm^2) and evenly spaced 0.2 (mm^2) as shown in Figure 3. These lateral displacement of patches over the RO 3035 substrate of thickness 1.5 (mm) ensures a lower Q-value, improves

bandwidth and form the multilayer antenna's first layer.

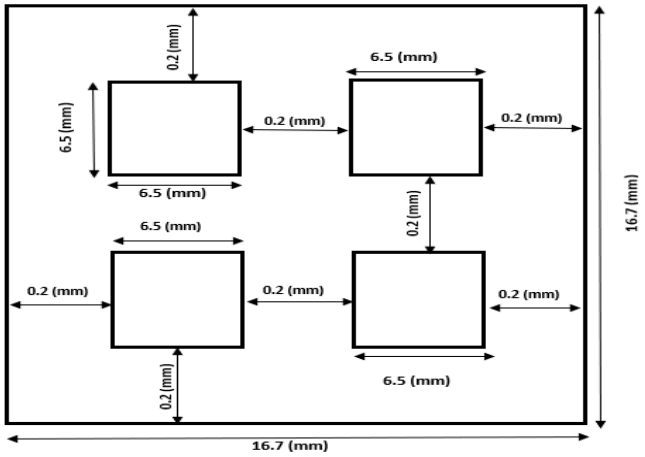

Figure 4. Four lateral displaced parasitic patches

Meander Line Slot Placement

Meander line slots act as reactive loads providing isolation between the radiating patches, thus reducing mutual coupling [23]. A meander line slot is itched on the lateral displaced parasitic patches to achieve isolation of < - 25 dB between the elements, as shown in Figure 4. The meander line comprises vertical and horizontal lines of dimensions 2 x 0.4 (mm^2) [23].

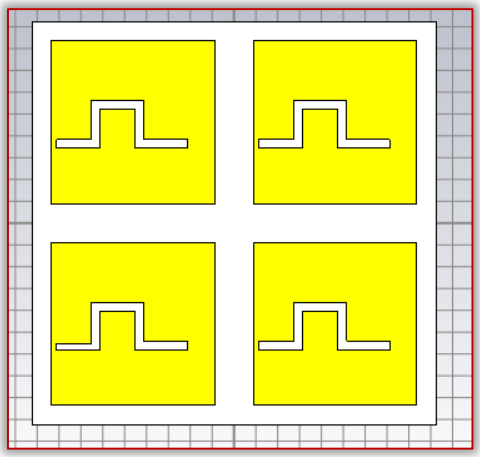

Figure 5. The Meander Line Slot itched on the Parasitic Patch

Substrate Selection

The substrates selected for the compact UWB patch antenna are RO 3035 and RO 4350B. Figure 5 shows the Rogers Corporation data sheets for the relative permittivity and loss tangent for RO 3000 series and RO 4000 series circuit materials. RO 3035 and RO 4350B were selected because of their lower relative permittivity (3.6 and 3.48), lower loss tangent (0.0015 and 0.0031) and better dimensional stability. To prevent surface wave loss, Equation (6) is used to determine the maximum allowable thickness of the multilayer antenna [15].

$$\frac{h}{\lambda} < \frac{0.3}{2\pi\sqrt{\epsilon r}} \quad (6)$$

where λ is the wavelength and h denotes the allowable height of the multilayer antenna.

Property	Typical Value[1]			
	RO3003	RO3035	RO3006	RO3010
Dielectric Constant, ε_r Process	3.00 ± 0.04	3.50 ± 0.05	6.15 ± 0.15	10.2 ± 0.30
[2] Dielectric Constant, ε_r Design	3.00	3.60	6.50	11.20
Dissipation Factor, tan δ	0.0010	0.0015	0.0020	0.0022
Thermal Coefficient of ε_r	-3	-45	-262	-395
Dimensional Stability	-0.06 0.07	-0.11 0.11	-0.27 -0.15	-0.35 -0.31

Property	Typical Value	
	RO4003C	RO4350B
Dielectric Constant, ε_r Process	3.38 ± 0.05	[1] 3.48 ± 0.05
[2] Dielectric Constant, ε_r Design	3.55	3.66
Dissipation Factor tan, d	0.0027 0.0021	0.0037 0.0031
Thermal Coefficient of ε_r	+40	+50

Figure 6. Rogers Corporation Data Sheet

Width of the microstrip Feed

The width of the feeding line depends on the height of the substrate, the dielectric constant and the thickness of the feeding strip [21]. This is important for maximum radiation intensity. The width of the feeding strip is given by Equation (7) [21].

$$W_f = \frac{7.48h}{e^{\left(Z_0\frac{\sqrt{\epsilon r}+1.41}{87}\right)}} - 1.25t \quad (7)$$

where W_f is the width of the feeding line, h is the height of the substrate, ϵr is the dielectric constant and t is the thickness of the feeding line.

Using the design concept in [15], a Via traversing layer two is used along with the feeding strip for optimal impedance tuning. This is depicted in Figure (6).

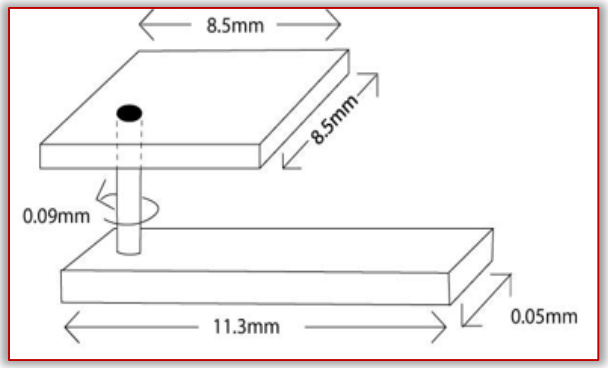

Figure 7. The Via, driven patch and strip line arrangement

To achieve a six-layer structure patch antenna, two copies of the complete subarray structure were created and placed back-to-back but rotated at 90 degrees to each other as shown in Figure 7. A central copper ground plane separates the two copies of the structure. Excited at its two ports, the structure produces two radiation pattern functions that are nearly

uncorrelated (i.e., mathematically orthogonal) and are suitable for diversity or MIMO use.

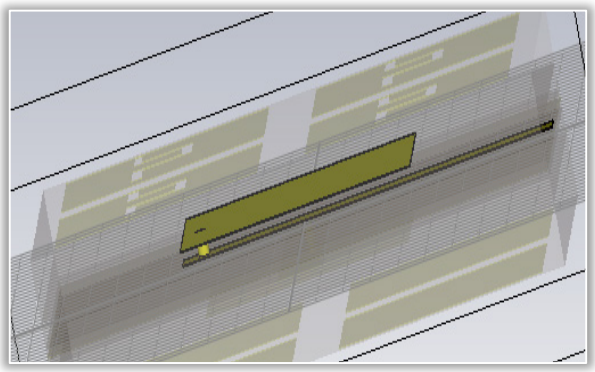

Figure 8. The simulated Via and Strip Line

To evaluate the performance of the UWB MIMO patch antenna, the percentage improvement and reduction of the improved compact UWB MIMO patch antenna over the compact diversity patch antenna in [15] is expressed using Equation (8) and Equation (9).

$$\%\ \text{metric Improvement} = \frac{\sum_{n=1}^{N}\left(\frac{\text{Modified Antenna}-\text{Original Antenna}}{\text{Original Antenna}}\right)}{N}\ X\ 100 \quad (8)$$

$$\%\ \text{metric Reduction} = \frac{\sum_{n=1}^{N}\left(\frac{\text{Original Antenna}-\text{Modified Antenna}}{\text{Original Antenna}}\right)}{N}\ X\ 100 \quad (9)$$

SIMULATION AND RESULTS

Using the mathematical model equations from Equation (1) to Equation (7), the dimensions of the various antenna parameters were calculated and tabulated in Table 1.

Table 1. Simulated Parameters

Parameters	Dimensions (mm)
Driven Patch Width	8.5
Driven Patch Length	8.5
Parasitic Patch Width	6.5
Parasitic Patch Length	6.5
Separation between Parasitic Patch	0.2
Antenna Width	16.7
Antenna Length	16.7
Via wrt to Driven Patch Center	2.95
1st Layer (RO 3035) Thickness	1.52
2nd Layer (RO 4350B) Thickness	0.76
3rd Layer (RO 3035) Thickness	0.25
Feeding Strip Width	0.5
Feeding Strip Length	11.3
The Diameter of the Via	0.09

RESULTS AND DISCUSSION

The results of the improved compact UWB MIMO multilayer patch antenna and the existing works were observed under the conditions of the reflection coefficient, the isolation between elements, ECC and the overall size of the antenna. A simulation was carried out using CST microwave studio to measure the antenna performance, and the graphs of the value generated were plotted as depicted in Figure 7 to Figure 9. The antenna performance metrics for comparison are the Reflection coefficient, ECC, mutual coupling, and size. The reductions and improvement for the performance metrics considered were determined using Equation (8) and Equation (9), summarized and represented in Table 2.

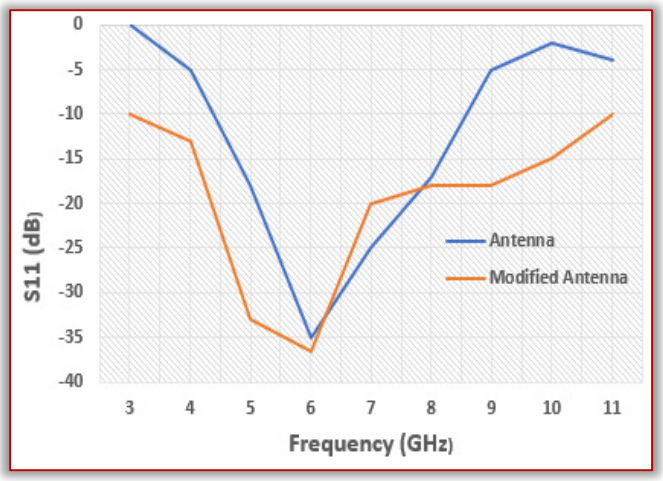

Figure 9. S11 Comparison of the Modified Antenna and Diversity Patch Antenna

The simulated result depicted in Figure 7 shows that the modified UWB MIMO antenna satisfies the accepted value of S11(< -10 dB) over a wider operational frequency range of 3 GHz – 11 GHz as against the 4 GHz bandwidth of the wideband diversity antenna [15].

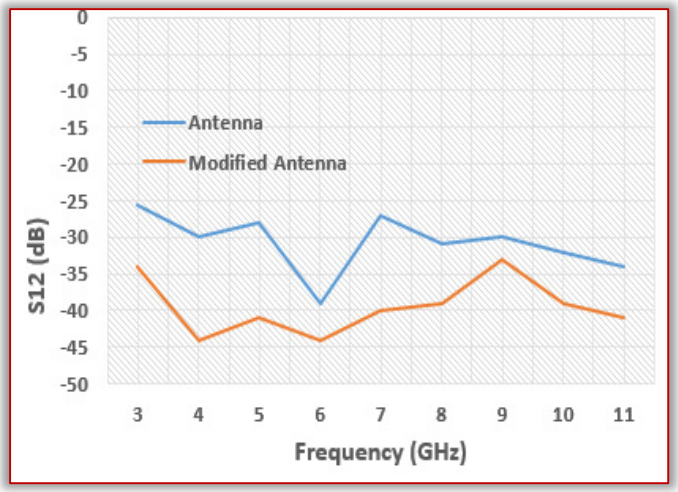

Figure 10. S12 Comparison of the Modified Patch Antenna and Diversity Patch Antenna

The simulated result depicted in Fig. 8 shows that the modified UWB MIMO antenna satisfies the

accepted value of S12(< -33 dB) over the operational frequency range of 3 GHz – 11 GHz.

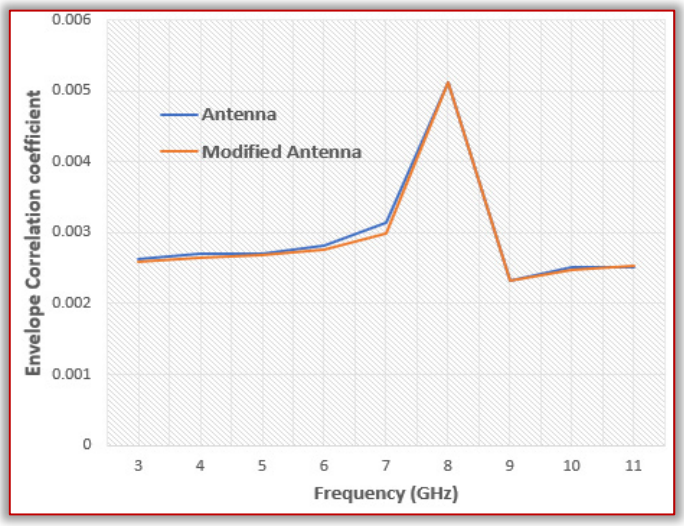

Figure 11. ECC Comparison of the Modified Patch Antenna and Diversity Patch Antenna

The simulated result depicted in Figure 8 shows that the modified UWB MIMO antenna satisfies the accepted value of S12(< 0.005) over the operational frequency range of 3 GHz – 11 GHz.

Validation

To Validate the improved UWB MIMO multilayer structure patch antenna, the percentage improvement and reduction of the improved antenna over the wideband diversity antenna is shown in Table 2.

Table 2: Percentage Reduction and Improvement Computation

Figures	Performance Metrics	Algorithm	Percentage Improvement (%)
Figure 8	Bandwidth	Modified UWB MIMO Patch Antenna compared with the Diversity patch antenna	97.5
Figure 9	Isolation	Modified UWB MIMO Patch Antenna compared with the Diversity patch antenna	28.4
Figures	Performance Metrics	Algorithm	Percentage Reduction (%)
Figure 10	ECC	Modified UWB MIMO Patch Antenna compared with the Diversity patch antenna	1.36
Figure 6	Size	Modified UWB MIMO Patch Antenna compared with the Diversity patch antenna	79.75

CONCLUSIONS

The demand for higher data rates has led to 5G wave systems. 5G radio signals suffer from multipath propagation due to reflection, diffraction and scattering. This phenomenon results in multipath fading which leads to signal attenuation.

This research study provides a compact two-port multilayer MIMO patch antenna that can mitigate multipath propagation through space diversity technique and provides a wide bandwidth for 5G wave applications. RO3035 and RO4350B substrates were selected for this research to achieve the desired antenna performance because of their low dielectric loss and low tangential loss.

For validation and comparison of this work, the results obtained were compared with existing work in terms of the bandwidth, isolation, envelope correlation coefficient and size where it outperforms the existing work by 97.5% bandwidth improvement, 28.40% isolation improvement, 79.75% size reduction, and 1.36% envelope correlation coefficient reduction.

References

[1] M. Farasat, D. N. Thalakotuna, Z. Hu, and Y. Yang, "A Review on 5G Sub-6 GHz Base Station Antenna Design Challenges," Electronics, vol. 10, no. 16, Art. no. 16, Jan. 2021

[2] L. Liu, W. Cheung, and T. I. Yuk, "Compact MIMO antenna for portable devices in UWB Applications," Antennas Propag. IEEE Trans. On, vol. 61, pp. 4257–4264, Aug. 2013.

[3] M. Farasat, D. N. Thalakotuna, Z. Hu, and Y. Yang, "A Review on 5G Sub-6 GHz Base Station Antenna Design Challenges," Electronics, vol. 10, no. 16, Art. no. 16, Jan. 2021.

[4] T. Kaiser, F. Zheng, and E. Dimitrov, "An overview of ultrawide-band systems with MIMO," Proceedings of the IEEE, vol. 97, no. 2, pp. 285–312, 2009.

[5] G. J. Foschini and M. J. Gans, "On limits of wireless communications in a fading environment when using multiple antennas," Wireless Personal Communications, vol. 6, no. 3, pp. 311–335, 1998

[6] S. Zhang, B. K. Lau, A. Sunesson, and S. He, "Closely-packed UWB MIMO/diversity antenna with different patterns and polarizations for USB dongle applications," IEEE Transactions on Antennas and Propagation, vol. 60, no. 9, pp. 4372–4380, 2012.

[7] G. Adamiuk, S. Beer, W. Wiesbeck, and T. Zwick, "Dual orthogonal polarized antenna for UWB-IR technology," IEEE Antennas and Wireless Propagation Letters, vol. 8, pp. 981– 984, 2009.

[8] A. Sabah and M. Jasim, "A new patch antenna for ultrawideband communication applications," Indones. J. Electr. Eng. Comput. Sci., vol. 18, p. 848, May 2020

[9] H. Alsaif and M. A. H. Eleiwa, "Compact Design of 2 × 2 MIMO Antenna with Super-Wide Bandwidth for Millimeters Wavelength Systems," Symmetry, vol. 13, no. 2, Art. no. 2, Feb. 2021

[10] H. AL-Saif, M. Usman, M. T. Chughtai, and J. Nasir, "Compact UltraWide Band MIMO Antenna System for Lower 5G Bands," Wirel. Commun. Mob. Comput., vol. 2018, p. e2396873, Jun. 2018

[11] D.-Y. Choi, "Study on Mutual Coupling Reduction Technique for MIMO Antennas," IEEE Access, vol. PP, pp. 1–1, Dec. 2018

[12] S. Zhang, B. Lau, A. Sunesson, and S. He, "Closely-Packed UWB MIMO/Diversity Antenna With Different Patterns and Polarizations for USB

Dongle Applications," IEEE Trans. Antennas Propag., vol. 60, pp. 4372–4380, Sep. 2012.

[13] L. Liu, W. Cheung, and T. I. Yuk, "Compact MIMO antenna for portable devices in UWB Applications," Antennas Propag. IEEE Trans. On, vol. 61, pp. 4257–4264, Aug. 2013

[14] T. Mandal and S. Das, "Bandwidth Enhancement of Stacked Microstrip Antennas Using Hexagonal Shape Multi-resonators," in Advances in Power Electronics and Instrumentation Engineering, V. V. Das, N. Thankachan, and N. C. Debnath, Eds., Berlin, Heidelberg: Springer, 2011, pp. 1–6

[15] M. Shishkin, "Bandwidth Enhancement Methods Analysis for High-gain Stacked Microstrip Antenna," Prog. Electromagn. Res. B, vol. 107, pp. 19–31, Jan. 2024

[16] S. R. K, R. G. S. N, and M. M, "Design and Implementation of a Miniaturised Microstrip Meander Line Antenna for X-Band Applications," Int. J. Electron. Commun. Eng., vol. Volume 11, May 2024

[17] O. Arabi et al., "Compact Wideband MIMO Diversity Antenna for Mobile Applications Using Multi-Layered Structure," Electronics, vol. 9, no. 8, Art. no. 8, Aug. 2020.

[18] S. I. Orakwue, "A Dual-band T-slot Microstrip Patch Antenna for Wireless Communication and Radar Application," J. Eng. Res. Rep., Apr. 2023, Accessed: Oct. 16, 2024. [Online]. Available: https://www.academia.edu/108471159/A_Dual_band_T_slot_Microstrip_Patch_Antenna_for_Wireless_Communication_and_Radar_Application

[19] S. K. Noor et al., "A Patch Antenna with Enhanced Gain and Bandwidth for Sub-6 GHz and Sub-7 GHz 5G Wireless Applications," Electronics, vol. 12, no. 12, Art. no. 12, J2023

[20] N. Shanmugam and S. v, "MIMO Antenna with Isolation Enrichment for 5G Mobile Information," Mob. Inf. Syst., vol. 2022, pp. 1–14, Feb. 2022.

[21] D. Marwa, C. Essid, and H. Sakli, "Muli-UWB Antenna System Design for 5G Wireless Applications with Diversity," Wirel. Commun. Mob. Comput., vol. 2021, pp. 1–18, Jun. 2021

[22] M. Z. Islam and M. Hussain, "Effect on Performance Characteristics of Patch Antenna for the Variation of Design Parameters," Oct. 2015.

[23] G. Jin, C. Deng, Y. Xu, J. Yang, and S. Liao, "Differential Frequency Reconfigurable Antenna Based on Dipoles for Sub-6GHz 5G and WLAN Applications," IEEE Antennas Wirel. Propag. Lett., vol. PP, pp. 1–1, Jan. 2020

[24] S. Aqeel et al., "A Dual-Band Multiple Input Multiple Output frequency agile antenna for GPS L1/Wifi/WLAN 2400/LTE Applications," Int. J. Antennas Propag., vol. 2016, Jan. 2016.

[25] S. R. K, R. G. S. N, and M. M, "Design and Implementation of a Miniaturised Microstrip Meander Line Antenna for X-Band Applications," Int. J. Electron. Commun. Eng., vol. Volume 11, May 2024

ISSN: 2067-3809